Chalcogenide Letters Vol. 17, No. 11, November 2020, p. 555 - 563

HYDROTHERMAL SYNTHESIS OF THE FLOWER-LIKE MoS_2 NANOSHEETS MICROSPHERES AND ITS PHOTOCATALYTIC DEGRADATION OF METHYL ORANGE

L. LIANG[a], Z. MO[b], N. LI[a], H. LIU[a], G. FENG[c], A. WEI[a,c,*]
[a]*School of Information Science, Xinhua College of Sun Yat-Sen University, Guangzhou 510520, China*
[b]*School of Biomedical Engineering, Xinhua College of Sun Yat-Sen University, Guangzhou 510520, China*
[c]*School of Material and Energy, Guangdong University of Technology, Guangzhou, 510006, China*

The flower-like MoS_2 microspheres were synthesized via a facile hydrothermal method using $Na_2MoO_4 \cdot 2H_2O$, $C_2H_2O_4 \cdot 2H_2O$, $SC(NH_2)_2$ and de-ionized water as precursors. The morphology and crystal structure of the MoS_2 microspheres were characterized using scanning electron microscope (SEM) and X-ray diffraction (XRD). The as-prepared MoS_2 microspheres were used as a catalyst for photocatalytic degradation of methyl orange. The effect of the size of the MoS_2 microspheres and catalyst dosage amount on photocatalytic activity were investigated. The results indicate that the MoS_2 powder consists of the flower-like nanosheet microspheres formed by several nanosheets gathered together perpendicular to the spherical surface, and the diameter of the MoS_2 microspheres decreases with increasing the concentration of oxalic acid in the precursor. The MoS_2 microspheres are with hexagonal 2H-MoS_2 structure and preferentially grow along the (002) plane. It is found that the best photocatalytic degradation efficiency is 79.0% within irradiation time of 120 min under MoS_2 dosage amount of 1.33 g/L and methyl orange concentration of 20mg/L.

(Received September 15, 2020; Accepted November 7, 2020)

Keywords: Hydrothermal method, MoS_2 nanosheets microspheres, Photocatalysis

1. Introduction

Synthetic dyes have been increasingly used in textiles, foodstuffs, paper, and leather industries for their production [1-2]. However, waste water pollutants discharged in the environment are highly hazardous and toxic, and are not biodegradable. In order to degrade these harmful dye pollutants in wastewater, in recent decades, people have tried to invest in various solutions, such as flocculation precipitation method, microbial decomposition method and photocatalytic degradation method etc. [3,4]. Among these methods, visible-light-driven semiconductor photocatalytic degradation is one of the most cost effective methods, and has

* Corresponding author: weiax@gdut.edu.cn

attracted significant attention, owing to its potential applications in eliminating organic pollutants [5-9].

Molybdenum disulfide (MoS_2) is a layered semiconductor composed of three layers of covalently bonded S-Mo-S, and the three layers (S-Mo-S) can be arranged in the following way: Hexagon (2H-MoS_2), Diamond (3R-MoS_2) and triangle (1T-MoS_2). However, the 2H-MoS_2 is an indirect band gap semiconductor with a band gap in the range of 1.2–1.8eV, which is an ideal visible light induced photocatalyst for solar energy utilization efficiently [10-12].

As we all know, the shape and size of MoS_2 have an important impact on its performance. At present, the complex nanostructure self-assembling materials are receiving more and more attention due to their unique properties and potential application compared to bulk materials. There are various methods to prepare MoS_2 material in recent years, such as chemical vapor deposition [13], electrostatic spinning [14], template method [15] and hydrothermal method [10]. Accordingly, various morphologies of MoS_2 were successfully prepared, such as nanowires [16], nanotubes [17], nanorods [18], the hollow microspheres [19], nanoflower [20, 21] and nanopolyhedron [22].

In this paper, the flower-like MoS_2 nanosheets microspheres were synthesized by hydrothermal method. The diameter of the MoS_2 microspheres was controlled by changing oxalic acid concentration in precursors. The photocatalytic activity of MoS_2 for degradation of methyl orange under exposure to visible light was studied. The effect of the size of MoS_2 nanosheets microspheres and catalyst dosage amount on photocatalytic activity were investigated. Moreover, a probable mechanism was proposed for describing the process of photocatalysis

2. Experiment details

2.1. Preparation of MoS_2 microspheres

Sodium molybdate（$Na_2MoO_4 \cdot 2H_2O$, thiourea（$SC(NH_2)_2$, oxalic acid（$C_2H_2O_4 \cdot 2H_2O$）were used as starting materials. All reagents are analytically pure and can be used without further purification. The synthesis process of the MoS_2 microspheres was summarized as follows: Firstly, 3 mmol of $Na_2MoO_4 \cdot 2H_2O$, 12 mmol $SC(NH_2)_2$ and 3 mmol $C_2H_2O_4 \cdot 2H_2O$ were dissolved and mixed in 40 ml of de-ionized water as the precursor solution. Oxalic acid ($C_2H_2O_4 \cdot 2H_2O$) as a surfactant plays an important role for the formation of the MoS_2 microspheres. The precursor solution was stirred for 20 min before the precursor solution became a transparent liquid; it was transferred to into 60 ml Teflon liner. Then, the Teflon liner was loaded in a stainless steel autoclave and heated in an oven. The hydrothermal reaction continues for 24 h at temperature of 200 °C. Finally, the autoclave was cooled to room temperature naturally. The sample was collected by centrifugation, washed several times with anhydrous ethanol and distilled water, and then dried under vacuum at 80 °C for 4 h. In order to prepared the MoS_2 microspheres with different diameter, the concentration of oxalic acid was changed from 0 M, 0.0375 M, and 0.0750 M to 0.1125 M, respectively, while the concentrations of other reaction reagents were kept constant. The different samples were denoted as A1, A2, A3 and A4. The deposition parameters were listed in Table 1.

Table 1. Deposition process parameters of various MoS_2 microspheres.

Samples No	$Na_2MoO_4 \cdot 2H_2O$ (M)	$SC(NH_2)_2$ (M)	$C_2H_4O_2 \cdot 2H_2O$ (M)	Water (ml)	Temperature (°C)	Time (h)
A1	0.075	0.3	0	40	200	24
A2	0.075	0.3	0.0375	40	200	24
A3	0.075	0.3	0.075	40	200	24
A4	0.075	0.3	0.1125	40	200	24

2.2. Characterization of the MoS_2 microspheres

The morphology of the as-synthesized MoS_2 powders was observed with a scanning electron microscope (SEM, S-3400, Hitachi). The crystal structure of the as-synthesized MoS_2 powders was characterized by X-ray diffraction (XRD, D / MAX-UltimalV, Rigaku).

2.3. Photocatalytic performance measurement of the MoS_2 microspheres

The MoS_2 microspheres prepared at different oxalic acid concentration were used as a photocatalytic material. The photocatalytic activities of the MoS_2 microspheres were investigated in terms of the photocatalytic degradation of the methyl orange at room temperature. First, the methyl orange aqueous solution with concentration of 20 mg/L was prepared. Second, 0.2 g of the MoS_2 microspheres was placed into a 150 mL methyl orange solution in a 250 mL beaker. In order to establish the adsorption-desorption equilibrium between the MoS_2 catalyst and the methyl orange solution, the solution was vigorously stirred in the dark for 5 min. All as-fabricated flower-like MoS_2 microspheres were evaluated under the same condition in order to study the effect of the size on photocatalytic activities. Third, a 500W Xe lamp was used as the simulated visible-light source. The distance between the light source and the beaker was approximately 30 cm. During light irradiation, 3 mL of mixed suspension solution was taken at a regular interval of 15 min using a syringe and after centrifugation to separate the catalyst. Finally, the absorbance of the degraded methyl orange solution was obtained using a UV-Vis spectrophotometer near to 463 nm which correspond to the characteristic absorption peak of methyl orange solution. The degradation efficiency of methyl orange was calculated according to the following formula

$$\eta = \frac{(A_0 - A_t)}{A_0} \times 100\% \quad (1)$$

Where η is the degradation efficiency, A_0 represents the absorbance of the initial methyl orange solution in absence of catalyst, A_t represents the absorbance of methyl orange solution at time t in the presence of a catalyst.

3. Results and discussion

3.1. Morphologies and structure of the MoS_2 microspheres

Fig. 1 displays the SEM images of the MoS_2 powders prepared using oxalic acid concentration of 0 M, 0.0375 M, 0.0750 M and 0.1125 M, respectively. It can be seen that the

MoS_2 powder is made of the flower-shaped microspheres formed by many nanosheets perpendicular to the spherical surface and gathered together. We could call these powders as "MoS_2 nanosheet microspheres". It can be observed that the size of the MoS_2 microspheres decreases with increasing the concentration of oxalic acid in the precursor. This indicates that the concentration of oxalic acid in the precursor has a significant effect on the diameter of MoS_2 microspheres. When the oxalic acid concentration is increased from 0 M, 0.0375M to 0.075M, the flower-like MoS_2 microspheres could be prepared successfully and the corresponding average diameter of the microspheres is about 4.6μm, 3.8μm, 1.6μm, respectively. However, when the concentration of oxalic acid was further increased to 0.1125M, the MoS_2 powder consisted of a large number of small particles with an average diameter of only about 0.25 μm.

Fig. 2 shows the XRD patterns of the MoS_2 powders (sample A3) prepared at oxalic acid concentration of 0.075 M. The major XRD diffraction peaks appeared at 2θ= 14.12°, 33.58°, and 58.80° can be indexed (002), (101) and (110) planes of hexagonal phase MoS_2 (JCPDS No.37-1492), respectively. No diffraction peaks of impurities are observed, indicating that the MoS_2 are a pure hexagonal phase. Furthermore, the X-ray diffraction patterns show that the intensity of (002) diffraction peak is stronger than that of other peaks, which is due to the stacking of single layers.

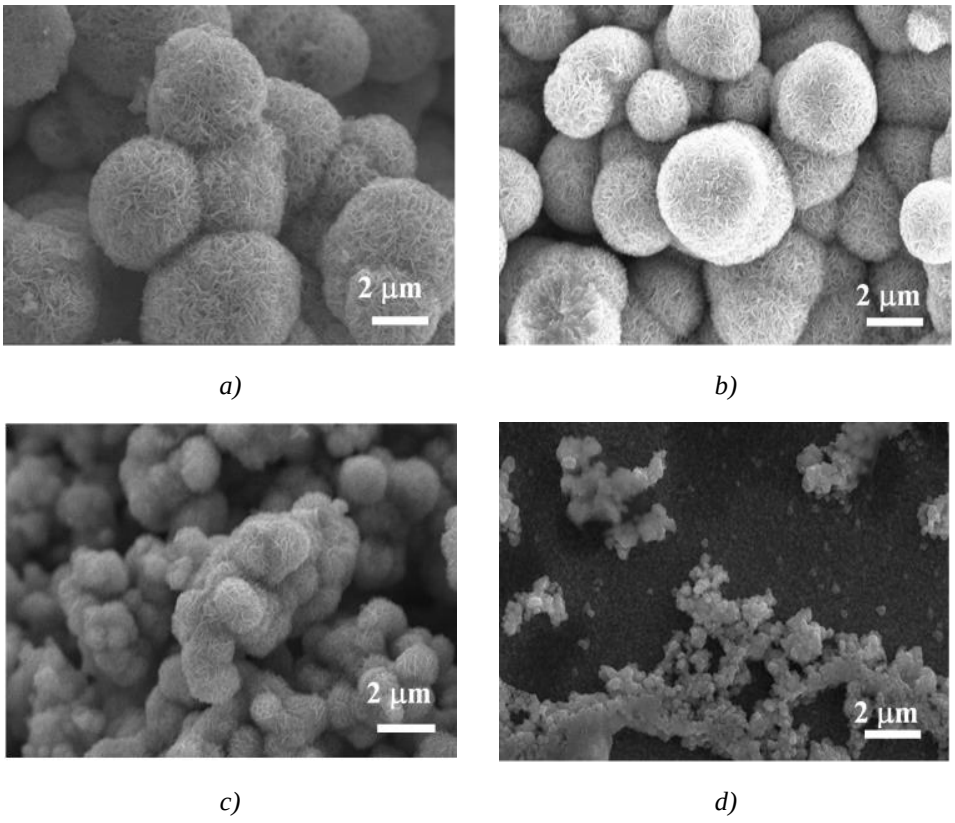

a) *b)*

c) *d)*

Fig. 1. SEM images of the MoS_2 powders prepared at 200℃ for 24h using different oxalic acid concentrations: a) 0 M; b) 0.375 M; c) 0.075 M; d) 0.1125 M.

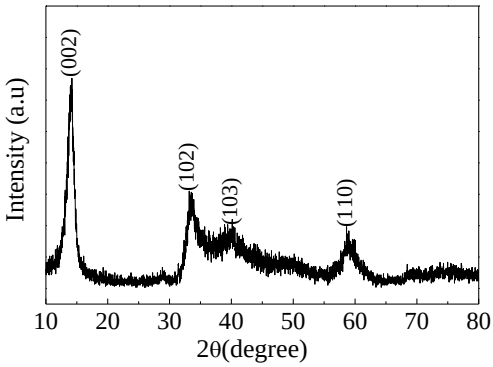

Fig. 2. XRD patterns of the MoS_2 microspheres *(sample A3) prepared at 200℃ for 24h.*

3.2. Photocatalytic performance of the MoS_2 microspheres

In order to investigate the photocatalytic performance of the MoS_2 microspheres with the different diameter, methyl orange was selected as the organic pollutant materials to be degraded under the visible light irradiation. Fig. 3a shows the UV-visible absorption spectra of methyl orange solution under solar light irradiation 15min using MoS_2 microspheres with different diameter as catalysts. Furthermore, to study the structural stability of methyl orange under the visible light irradiation, the pure methyl orange solution without any catalyst addition is also tested at the same. Compared with the pure methyl orange solution without any catalyst, the absorbance at 463 nm of the methyl orange solution with different diameter MoS_2 catalyst is decrease significantly. The degradation efficiency of methyl orange calculated according to the formula (1) as function of irradiation time is depicted in Fig. 3b. The degradation efficiency η is used to evaluate the catalytic activity of the MoS_2 catalyst. For comparison, the degradation curve of methyl orange solution without any catalyst is also shown in the Figure 3b. It can be found that the degradation of methyl orange is negligible in the absence of a catalyst, suggesting that methyl orange is structural stability and cannot be degraded under visible light irradiation. As expected, in the presence of the MoS_2 catalyst, the MoS_2 catalyst exhibits photocatalytic performance toward methyl orange degradation. However, as illustrated in Fig. 3b, the microstructure of MoS_2 has obvious effect on photocatalytic degradation efficiency of methyl orange. Among the four catalysts A1, A2, A3 and A4，the photocatalytic activity of A3 and A4 are superior than that of A1 and A2. For the catalysts A3 and A4, the photocatalytic degradation efficiency gradually increased with the extension of illumination time, reaching 79% and 60.6% when illumination time is 120 min, respectively. The degradation efficiency of catalysts A1 and A2 is not only relatively low, but also it increases very slowly with the increase the illumination time. The degradation efficiency of A1 and A2 is only about 10.6% and 13.6% when illumination time is 120 min, respectively. The A3 catalyst exhibits the best photocatalytic efficiency，which can be attributed to its flower-like shape and smaller diameter of MoS_2 microspheres. As can be seen from Fig. 1, the flower-like MoS_2 microspheres are formed by many nanosheets gathering together perpendicular to the spherical surface, and the average diameter of samples A1, A2 and A3 is about 4.6μm, 3.8μm, 1.6μm, respectively. The smaller the diameter of the microspheres, the larger the specific surface area is. The large specific surface area of the MoS_2 microspheres increase the contact area between MoS_2 catalysts and methyl orange solution, which is conducive to enhancing the number of

surface active groups and improving the electronic transmission speed of MoS_2 catalyst. Therefore, A3 catalyst has a higher degradation rate to the methyl orange than A1 and A2. In addition, although A4 catalyst has the smallest diameter (0.25 μm), but it no longer has the flower-like morphology which results in the specific surface area is smaller than that of A3 catalyst. Therefore, the photocatalytic degradation efficiency of A4 catalyst is lower than that of A3 catalyst.

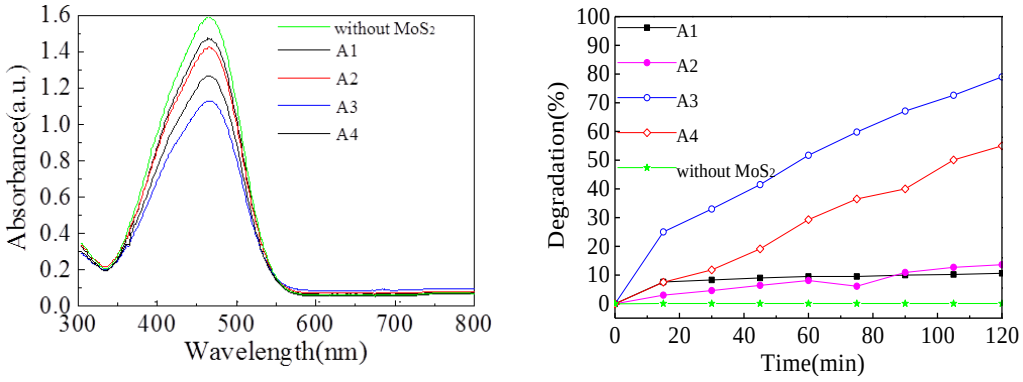

a) *b)*

Fig. 3. (a) UV-visible absorption spectrum of methyl orange solution under solar light irradiation 15min using MoS_2 microspheres with different diameter as catalysts; (b) Photocatalystic degradation efficiency of methyl orange in the presence of MoS_2 microspheres with different diameter.

Catalyst dosage is an important parameter to affect the efficiency of the photocatalytic reaction. To study effect of the catalyst dosage on photocatalytic degradation efficiency, the photo-degradation experiments are carried out using four different catalyst dosage of 0.67 g/L, 1.00 g/L, 1.33 g/L and 1.67 g/L, respectively, at methyl orange concentration of 20mg/L. The results are shown in Fig. 4a. In this photo-degradation experiments, MoS_2 (A3) prepared at oxalic acid concentrations of 0.0750 M is used as catalyst. It can be observed that the amount of MoS_2 catalyst increased from 0.67g / L to 1.33g / L, and the degradation rate increased from 46.7% to 79.0%. However, when the amount of MoS_2 is further increased to 1.67g / L, the degradation rate will drop to 62.5%. Excessive MoS_2 will lead to a reduction in degradation efficiency, which may be caused by shadow effects and increased opacity. When the catalyst is excessive, more solid will be suspended in the aqueous solution, which hinders the effective transmission and absorption of light, so that the light energy cannot be effectively absorbed by the catalyst, that is to say, the catalyst is not fully utilized. In addition, high concentrations of MoS_2 can cause severe agglomeration, thereby reducing the charge transfer ability. It can be concluded that the catalyst dosage amount has obviously effect on photocatalytic degradation efficiency, The MoS_2 dosage amount of 1.33 g/L has stronger catalytic effect, and its photocatalytic degradation efficiency is 79.0% within 120min of irradiation time.

In order to determine the proper methyl orange concentration, the photo-degradation experiments are conducted using four different methyl orange concentration of 10 mg/L, 20 mg/L, 30 mg/L and 40 mg/L, respectively at MoS_2 catalyst dosage of 1.33 g/L. The results are presented in Figure 4b. When irradiation time is 120 min, the photocatalytic degradation efficiency reaches to 68.1%, 79.0%。44.2% and 14.9% for methyl orange concentration of 10 mg/L, 20 mg/L, 30

mg/L and 40 mg/L, respectively. It is found that the degradation efficiency is smaller for methyl orange concentration of 10 mg/L than of 20 mg/L. Generally speaking, the less the concentration of methyl orange, the easier it is to degrade. However, when the concentration of methyl orange is degraded to a certain extent, the degradation reaction between the MoS_2 catalyst and methyl orange will reach equilibrium. Thus, it leads to the degradation efficiency smaller for methyl orange concentration of 10 mg/L than of 20 mg/L. When the concentration of methyl orange is increased from 20 mg/L to 40 mg/L, the photocatalytic degradation efficiency of the methyl orange gradually reduce. One possible explanation for this phenomenon is that with the increase of methyl orange concentration, a large amount of light may be absorbed by methyl orange molecules, rather than by MoS_2 catalyst, resulting in the reduction of the production of active substances. The result indicated that the best degradation efficiency is 79.0% at MoS_2 dosage amount of 1.33 g/L and methyl orange concentration of 20mg/L.

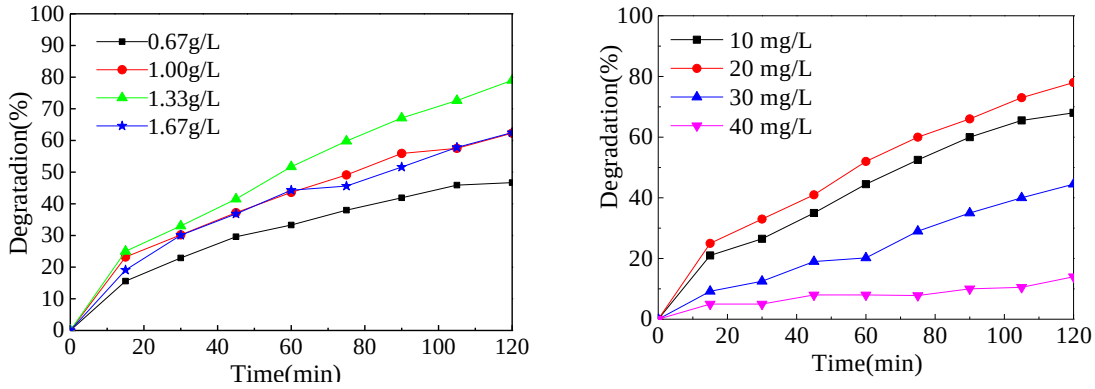

a) *b)*

Fig. 4. photocatalytic degradation efficiency (a) The methyl orange concentration is 20mg/L and the MoS_2 catalyst dosage (sample A3) is 0.67,1.00,1.33 and 1.67g/L,respectively; (b) The MoS_2 catalyst dosage is 1.33 g/L and the methyl orange concentration is 10,20,30 and 40 mg/L.

3.3. Photocatalytic degradation mechanism

Fig. 5 is the photocatalytic degradation mechanism of methyl orange, as shown in the following (2) - (6) expression. Under the visible light irradiation, the electrons in MoS2 are excited from valence band VB to conduction band CB by absorbing photons with energy larger than band gap, and the electron hole pairs are produced on the surface of MoS2 microspheres [4, 23]. On one hand, the excited electrons (ecb-) are captured by oxygen molecule (O2) to produce various reactive species, such as superoxide (·O2-), hydrogen peroxide (H2O2) and hydroxyl (·OH) radicals (Eq. (3-5)) [1, 24]. On the other hand, the positively charged holes (hvb+) will be formed under visible light, which has strong oxidizability, and some of them can directly conduct the oxidative degradation of the methyl orange dye. Besides, another part of the holes (hvb+) acting on the adsorbed water (H2O) and OH- in the MO solution, consequently form the hydroxyl (·OH) radicals (Eq. (6-7)) [25, 26] Noteworthiness, the hydroxyl (·OH) radicals is a powerful oxidizing agent, which can degrade the methyl orange molecules into environmentally friendly small molecules, such as H2O, CO2 (Eq. (8)) [27, 28]

$$MoS_2 + hv \rightarrow MoS_2 (h_{vb}^+ + e_{cb}^-) \quad (2)$$

$$e_{cb}^- + O_2 \rightarrow \cdot O_2^- \quad (3)$$

$$\cdot O_2^- + 2H^+ + e_{cb}^- \rightarrow H_2O_2 \quad (4)$$

$$H_2O_2 + e_{cb}^- \rightarrow 0H^- + \cdot OH \quad (5)$$

$$h_{vb}^+ + H_2O \rightarrow H^+ + \cdot OH \quad (6)$$

$$h_{vb}^+ + OH^- \rightarrow \cdot OH \quad (7)$$

$$\cdot OH + MO \rightarrow CO_2 + H_2O \quad (8)$$

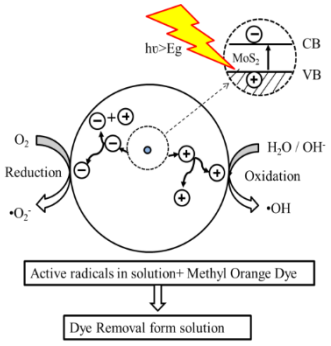

Fig. 5. Schematic illustration of the MoS_2 microspheres for photocatalytic degradation under the irradiation of visible light.

4. Conclusions

In summary, the flower-like MoS_2 nanosheets microspheres were successfully prepare using hydrothermal method. The MoS_2 microspheres with hexagonal 2H-MoS_2 structure are formed by several nanosheets gathering together perpendicular to the spherical surface. The diameter of the MoS_2 nanosheets microspheres decreases from 4.6 μm to 0.25 μm when the oxalic acid concentration in the precursors is increased from 0 M to 0.1125 M. The catalytic ability of the MoS_2 nanosheets microspheres with different diameter was studied in terms of photo-degradation of methyl orange. The diameter of MoS_2 MoS_2 nanosheets microspheres, MoS_2 catalyst dosage and methyl orange concentrations have a significant impact on photocatalytic degradation efficiency of methyl orange. The best degradation efficiency is 79.0% under MoS_2 dosage amount of 1.33 g/L and methyl orange concentration of 20mg/L after being exposed to light irradiation for 120 min. The MoS_2 photocatalyst displayed outstanding photocatalytic activity due to effective separation of photogenerated electrons and holes.

Acknowledgements

The authors gratefully acknowledge financial support from the Key Platforms and Scientific Research Projects of Guangdong Province (No. 2018KQNCX365).

References

[1] P. C. Dey, R. Das, Spectrochim. Acta. A Mol. Biomol. Spectrosc. **231**, 118122 (2020).
[2] E. Haque, J. W. Jun, S. H. Jhung, J. Hazard. Mater. **185**, 507 (2011).
[3] H. Liu, T. Lv, X. Wu, C. Zhu, Z. Zhu, Appl. Surf. Sci. **305**, 242 (2014).
[4] F. P. Yang, Z.Y. Zhang, Y. N. Wang, M. Z. Xu, W. Zhao, J. F. Yan, C. Chen, Mater. Res. Bull. **87,** 119 (2017).
[5] B. B. Sheng, J. S. Liu, Z.Q. Li, M. H. Wang, K. J. Zhu, J. H. Oiu, J. Wang, Mater. Lett. **144**, 153 (2015).
[6] J. Tian, Y. Leng, H. Cui, H. Liu, J. Hazard. Mater. **299**, 165 (2015).
[7] Y. M. Hunge, A. A. Yadav, V. L. Mathe, Ultrason. Sonochem. **45**, 116 (2018).
[8] N. M. Mahmoodi, J. Abdi, M. O. Mokhtar, A. Asli, M. Vossoughi, Mater. Res. Bull. **100**, 357 (2018).
[9] L. Dashairya, M. Sharma, S. Basu, P. Saha, J. Alloys Compd. **774**, 625 (2019).
[10] G. B. Feng, A. X. Wei, Y. Zhao, J. Liu, J. Mater. Sci: Mater. Electron. **26**, 8160 (2015).
[11] K. F. Mak, C. Lee, J. Hone, Phy. Rev. Lett. **105**, 136805 (2010).
[12] Z. H. Zhou, Y. L. Lin, P. Z. Zhang, E. Ashalley, M. Shafa, H. D. Li, J. Wu, Z. M. Wang, Mater. Lett. **131**, 122 (2014).
[13] I. Endler, A. Leonhardt, U. König, H. van den Berg, W. Pitschke, V. Sottke, Surf. Coat. Tech. **120**, 482(1999).
[14] S. H. Liu, X. B. Zhang, H. Shao, J. Xu, F. Y. Chen, Y. Feng, Mater Lett. **73**, 223 (2012).
[15] B. L. Hu, X.Y. Qin, A. M. Asiri, K. A. Alamry, A. O. Al-Youbi, X. P. Sun, Electrochim. Acta. **100**, 24 (2013).
[16] W. J. Li, E. W. Shi, J. M. Ko, Z. Z. Chen, H. Ogino, T. Fukuda, J. Cryst. Growth **250**, 418 (2003).
[17] Y. Tian, Y. He, Y. F. Zhu, Mater. Chem. Phys. **87**, 87 (2004).
[18] H. T. Lin, X. Y. Chen, H. L. Li, M. Yang, Y. X. Qi, Mater Lett. **64**, 1748 (2010).
[19] M. Wang, G. D. Li, H. Y. Xu, Y. T. Qian, J. Yang, ACS Appl. Mater. Interfaces **5**, 1003 (2013).
[20] L. R. Hu, Y. M. Ren, H. X. Yang, Q. Xu, ACS Appl. Mater. Interfaces, **6**, 14644 (2014).
[21] K. Pandey, P. Yadav, I. Mukhopadhyay, Rsc Advances. **5**, 57943 (2015).
[22] L. Ye, W. Guo, Y. Yang, Y. F. Du, Y. Xie, Chem. Mater. **19**, 6331 (2007).
[23] W. P. Zhang, X.Y. Xiao, L. L. Zheng, C. X. Wan, Can. J. Chem. Eng. **93**, 1594 (2015).
[24] W. Ho, J. C. Yu, J. Yu, P. Li, Langmuir **20**, 5865 (2004).
[25] S. Zhuang, X. Xu, B. Feng, J. Hu, Y. Pang, G. Zhou, L. Tong, Y. Zhou, ACS Appl. Mater. Interfaces **6**, 613 (2014).
[26] B. Tryba, M, Tygielska, C. Colbeau-Justin, E. Kusiak-Nejman, J. Kapica-Kozar, R. Wróbel, G. Zolnierkiewicz, N. Guskos, Mater. Res. Bull. **84**, 152 (2016).
[27] K. H. Hu, X. G. Hu, Y. F. Xu, X. Z. Pan, React. Kinet. Mech. Catal. **100**, 153 (2010).
[28] J. P. Wilcoxon, J. Phys. Chem. B **104**, 7334 (2000).